



## On the aero-elastic design of the DTU 10MW wind turbine blade for the LIFES50+ wind tunnel scale model

Bayati, I.; Belloli, M.; Bernini, L.; Mikkelsen, Robert Flemming; Zasso, A.

*Published in:*  
Journal of Physics: Conference Series (Online)

*Link to article, DOI:*  
[10.1088/1742-6596/753/2/022028](https://doi.org/10.1088/1742-6596/753/2/022028)

*Publication date:*  
2016

*Document Version*  
Publisher's PDF, also known as Version of record

[Link back to DTU Orbit](#)

*Citation (APA):*  
Bayati, I., Belloli, M., Bernini, L., Mikkelsen, R. F., & Zasso, A. (2016). On the aero-elastic design of the DTU 10MW wind turbine blade for the LIFES50+ wind tunnel scale model. *Journal of Physics: Conference Series (Online)*, 753, [022028]. <https://doi.org/10.1088/1742-6596/753/2/022028>

---

### General rights

Copyright and moral rights for the publications made accessible in the public portal are retained by the authors and/or other copyright owners and it is a condition of accessing publications that users recognise and abide by the legal requirements associated with these rights.

- Users may download and print one copy of any publication from the public portal for the purpose of private study or research.
- You may not further distribute the material or use it for any profit-making activity or commercial gain
- You may freely distribute the URL identifying the publication in the public portal

If you believe that this document breaches copyright please contact us providing details, and we will remove access to the work immediately and investigate your claim.

## On the aero-elastic design of the DTU 10MW wind turbine blade for the LIFES50+ wind tunnel scale model

This content has been downloaded from IOPscience. Please scroll down to see the full text.

2016 J. Phys.: Conf. Ser. 753 022028

(<http://iopscience.iop.org/1742-6596/753/2/022028>)

View [the table of contents for this issue](#), or go to the [journal homepage](#) for more

Download details:

IP Address: 192.38.90.17

This content was downloaded on 08/12/2016 at 13:14

Please note that [terms and conditions apply](#).

You may also be interested in:

[Large Wind Turbine Rotor Design using an Aero-Elastic / Free-Wake Panel Coupling Code](#)  
Matias Sessarego, Néstor Ramos-García, Wen Zhong Shen et al.

[Aerodynamic and Structural Design of MultiMW Wind Turbine Blades beyond 5MW](#)  
B Hillmer, T Borstelmann, P A Schaffarczyk et al.

[OC3—Benchmark Exercise of Aero-elastic Offshore Wind Turbine Codes](#)  
P Passon, M Kühn, S Butterfield et al.

[Aerofoil flutter: fluid-mechanical analysis and wind tunnel testing](#)  
A L Wensuslaus and A J McMillan

[Operating wind turbines in strong wind conditions by using feedforward-feedback control](#)  
Ju Feng and Wen Zhong Sheng

[Static behaviour of a laminated composite spherical shell cap with piezoelectricactuators](#)  
K S Sai Ram and S Kranthi Kiran

[Structural Load Analysis of a Wind Turbine under Pitch Actuator and Controller Faults](#)  
Mahmoud Etemaddar, Zhen Gao and Torgeir Moan

[Wind Turbine Model and Observer in Takagi-Sugeno Model Structure](#)  
Sören Georg, Matthias Müller and Horst Schulte

[Fault-Tolerant Control of Wind Turbines using a Takagi-Sugeno Sliding Mode Observer](#)  
Sören Georg and Horst Schulte

# On the aero-elastic design of the DTU 10MW wind turbine blade for the LIFES50+ wind tunnel scale model

I. Bayati<sup>1\*</sup>, M. Belloli<sup>1</sup>, L. Bernini<sup>1</sup>, R. Mikkelsen<sup>2</sup>, A. Zasso<sup>1</sup>

<sup>1</sup>Politecnico di Milano, Department of Mechanical Engineering, Milan, Italy

<sup>2</sup>Technical University of Denmark, Fluid Mechanics, Department of Wind Energy, Lyngby

E-mail: [ilmasandrea.bayati@polimi.it](mailto:ilmasandrea.bayati@polimi.it) \*, [marco.belloli@polimi.it](mailto:marco.belloli@polimi.it),  
[luca.bernini@polimi.it](mailto:luca.bernini@polimi.it), [rfmi@dtu.dk](mailto:rfmi@dtu.dk), [alberto.zasso@polimi.it](mailto:alberto.zasso@polimi.it)

**Abstract.** This paper illustrates the aero-elastic optimal design, the realization and the verification of the wind tunnel scale model blades for the DTU 10 MW wind turbine model, within LIFES50+ project. The aerodynamic design was focused on the minimization of the difference, in terms of thrust coefficient, with respect to the full scale reference. From the Selig low Reynolds database airfoils, the SD7032 was chosen for this purpose and a proper constant section wing was tested at DTU red wind tunnel, providing force and distributed pressure coefficients for the design, in the Reynolds range 30-250 E3 and for different angles of attack. The aero-elastic design algorithm was set to define the optimal spanwise thickness over chord ratio ( $t/c$ ), the chord length and the twist to match the first flapwise scaled natural frequency. An aluminium mould for the carbon fibre was CNC manufactured based on B-Splines CAD definition of the external geometry. Then the wind tunnel tests at Politecnico di Milano confirmed successful design and manufacturing approaches.

## 1. Introduction

Lifes50+ [1] project is an EU H2020 project which aims at proving cost effective technology for floating substructures for 10MW wind turbines, at water depths greater than 50 m. The objective is optimizing and qualifying, to a Technology Readiness Level (TRL) of 5, two innovative substructure designs for 10MW wind turbines, as well as developing a streamlined and a key performance indicator KPI based methodology for the evaluation and qualification process of floating substructures. A series of substructures are going to be tested in wind tunnel and ocean basin testing facilities as support platforms for a reference 10 MW wind turbine selected to be the one developed by DTU [2].

In order to perform the wind tunnel tests a scale model of the reference turbine was designed and constructed by the authors of this work, a good review of the similar past projects related to offshore wind turbine testing could be found in [3]. In this document it is highlighted that the main limitation in the rotor scaling procedure is the impossibility of matching the Reynolds number. A deep analysis of the scaling effect can be found in [4] regarding previous activities at Politecnico di Milano wind tunnel, this work deals with the definition of a procedure for aeroelastic model design, good results, in term of thrust and torque value matching were



obtained, as well as a correctly scaled blade structural behaviour also considering bend-twist scaling [5].

A further study on the scaling effect of the turbine rotor aerodynamics was carried out by Make [6] from TUDelft, the author found, both numerically and experimentally, that the Reynolds discrepancy caused a different behaviour of the model scale rotor. Make found that, by adjusting the chord length by an increment of 25%, the model rotor with the chord increment matched scaled thrust but not the power output value.

Similar results were obtained by DTU in [7], also in this case the rotor blades were geometrically adjusted in order to overcome the Reynolds scaling limit which, together with the use of low Reynolds airfoil and turbulence generators allowed to obtain good results for the rotor aerodynamic performances.

The Reynolds scaling problem is even more important when dealing with offshore related testing, in this case Froude scaling is mandatory [3], worsening further the Reynolds mismatch. For this reason Lifes50+ projects implements a novel experimental approach to test floating wind turbines, with the main goal to overcome Froude scaling issues. The approach consists in the Hardware-In-The-Loop hybrid testing approach where the motion of the scale model being tested is given simulated in real-time with a 6 DoF robot [?, 9].

This paper illustrates the aero-elastic optimal design, the realization and the verification of the wind tunnel scale rotor of the DTU 10 MW wind turbine, with offshore wind application purpose

## 2. Scaling of the reference design

The DTU 10 MW was firstly designed in the framework of the Light Rotor project in 2012 [11], starting from the upscaling of the reference 5MW turbine from NREL [12]. Later the Light Rotor project design evolved in the nowadays public available reference design from the DTU wind energy department. The DTU 10 MW is very often used as reference design in numerous research activities related to wind energy development, ranging from wind farm optimization to offshore wind turbine simulation or also for numerical tools benchmark and testing.

The first step of model design was the comparison between the turbine specifications and the Polimi Wind Tunnel (GVPM) [13] test section dimension and flow performances. The GVPM is a closed circuit facility with two tests rooms: a 4x4m high speed low turbulence and a 14x4m low speed boundary layer test section. The high speed section is characterized from very low turbulence,  $Iu < 0.15\%$ , and high speed, max velocity 55 m/s, in the low speed section the turbulence index is higher,  $Iu < 2\%$ , with a reduced maximum velocity, 15 m/s. The low speed section has the relevant dimension of 36m length, 14m width and 4m height, allowing for very large scale wind engineering simulations, useful for civil engineering application or low blockage aerodynamic related tests. Trying to avoid an excessive difficult miniaturization of the turbine model components the wind tunnel tests are performed in the low speed section.

In Eq. 1 the scale factor is defined as the ratio between a general DTU 10 MW turbine parameter and the corresponding wind tunnel model parameter.

$$\lambda = \frac{p_{reference}}{p_{model}} \quad (1)$$

Usually in wind tunnel testing the model design is based on the dimensional analysis technique, so that a series on non-dimensional group are usually taken into account, the most used are the Reynolds number, Froude Number, Strouhal Number, Cauchy number, etc. Usually the length scale,  $\lambda_L$ , is defined from simple considerations about the wind tunnel dimension, then one of the non-dimensional group is selected to be kept fixed from full scale to model scale. The choice is made considering which are the most important parameters that influence tests

results, for example Reynolds number have a strong influence in streamlined body aerodynamics or Froude number strongly affects aeroelastic response of slender structure like bridges.

Lifes50+ project goal is the simulation of floating system dynamics, this enforces the Froude scaling in order to correctly reproduce the hydrodynamic effect on the floater motion [3]. The HIL approach of using actuators to simulate the hydrodynamics behaviour of the turbine substructure permits to overcome Froude matching constraint allowing for a free selection of the velocity scale,  $\lambda_V$ .

For this particular project the  $\lambda_L$  has to be selected in the range: 70 – 90, the lower limit comes from the maximum wind tunnel model diameter of 2.5 m, this ensures that the blade tip is far enough from the tunnel ceiling and floor during the rotor revolution, thus avoiding the wall boundary layer. The higher limit avoid to have an excessive miniaturization of the model components.

The  $\lambda_V$  has a fixed range of possible values: 1.5 – 3 due to a comparison between the cut out speed, 25 m/s of the DTU 10 MW and the maximum wind tunnel speed, 15 m/s.

A discrete number of possible combinations for the scales were evaluated, a good compromise was found in  $\lambda_L = 75$  and  $\lambda_V = 2$ . Once defined the length and velocity scales, the scales of the principal physical quantities could be derived from dimensional analysis. Table 1 reports the most important scaled turbine characteristics.

Table 1: Wind Tunnel Model turbine specifications

Parameter	value	units	scale
Cut in wind speed	2	m/s	$\lambda_V = 2$
Cut out wind speed	12.5	m/s	$\lambda_V = 2$
Rated wind speed	5.7	m/s	$\lambda_V = 2$
Rotor Diameter	2.37	m	$\lambda_L = 75$
Maximum Rotor Speed	360	rpm	$\lambda_f = \lambda_L \lambda_V^{-1} = 37.5$
Rotor Mass	0.54	kg	$\lambda_M = \lambda_L^3 = 4.22 \cdot 10^5$

Beside the value in the table the blade design aims of matching as close as possible the scaled value for the turbine aerodynamic thrust and torque. It is worth mentioning that, since this scaled design is related to the study of a floating system, the thrust matching is of higher importance since the floating system dynamic more influenced by thrust than torque [7].

### 3. Wind Tunnel Model blade design Input

In this scenario, the main goals in the blade design can be summarized as follows:

- matching the reference thrust coefficient
- matching the scaled first blade flapwise frequency
- matching the scaled blade weight

It is pretty clear that the blade design is challenging both from an aerodynamic and a structural point of view. The blade has to be aero-elastically scaled from the reference one, the input of the scaling process are described in this section.

#### 3.1. Reference Design Input

The DTU 10 MW value regarding the turbine blade are publicly available, e.g. the chord, twist angle and relative thickness.

The reference and model turbine operational parameters are reported in Table 2, as combinations of wind speed,  $V$ , rotor rotational speed,  $\Omega$  and Tip Speed Ratio, TSR ( $TSR =$

$\Omega \cdot R/V$ ). The model wind speed operational value are reduced by  $\lambda_V$  and the model rotational speed is reduced by  $\lambda_V/\lambda_L$  this ensure that the TSR remains constant when scaling to wind tunnel dimension. Constraining the reference and model turbine of having the same values of TSR ensures to have the same aerodynamic kinematics, as it is going to be discussed in detail further on.

Table 2: Wind turbine operational parameters, V (m/s),  $\Omega$  (RPM) and TSR (-)

V(10MW)	$\Omega$ (10MW)	TSR(10MW)	V(model)	$\Omega$ (model)	TSR(model)
4.0	6.0	14.0	2.0	225.0	14.0
8.0	6.4	7.5	4.0	240.9	7.5
11.0	8.8	7.5	5.5	331.4	7.5
16.0	9.6	5.6	8.0	360.0	5.6
20.0	9.6	4.5	10.0	360.0	4.5
24.0	9.6	3.7	12.0	360.0	3.7

The 10 MW blade has a mass of 41.716 kg that leads to a scaled mass of about 0.1 kg, also the structural performances of the DTU 10MW blade are reported in Table 3.

Table 3: Reference structural permanences

Mode	reference frequency (Hz)	scaled frequency (Hz)
<b>1st flap mode</b>	<b>0.61</b>	<b>22.87</b>
1st edge mode	0.93	34.87
2nd flap mode	1.74	65.25
2nd edge mode	2.76	103.50

### 3.2. Model Airfoil

One of the most critical aspect in the model blade design is the airfoil selection, as a matter of fact the main limitation in reproducing the reference aerodynamic performances is related to the Reynolds number reduction when working at wind tunnel scales.

In Eq 2,  $\rho$  is the air density,  $U$  is the wind speed,  $c$  is the blade chord length and  $\mu$  is the air dynamic viscosity. The scale factor for Reynolds number is therefore defined as  $\lambda_{Re} = \lambda_L \lambda_V$  equal to 150 (i.e. the wind tunnel Reynolds is 150 times smaller the the full scale one). This could result in a completely different aerodynamic behaviour of the blade profile at model scale.

$$Re = \frac{\rho \cdot U \cdot c}{\mu} \quad (2)$$

$$\Lambda_{Re} = \Lambda_U \Lambda_L$$

The Reynolds discrepancy forces to use different airfoil shape than the one used by DTU. In particular the authors choice went on the SD70xx airfoil family from the Selig-Donovan low Reynolds database [14]. From similar previous experience [7], the selected airfoil was the SD7032, Fig.1 reports the model airfoil shape and the DTU 10MW blade tip one. The SD7032 has a thickness, i.e. the airfoil extension in y direction, of roughly 10% while the FFA-W3-240 thickness is 24%. The lower thickness leads to limited structural performances but it also makes the airfoil less sensible to flow separation at low Reynolds value conditions, like the ones encountered in the wind tunnel testing.

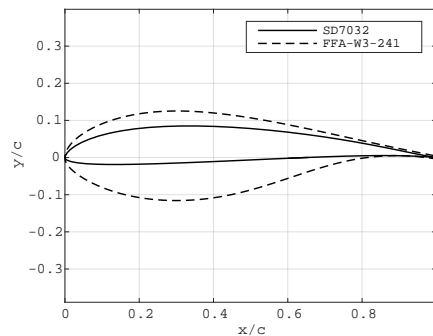


Figure 1: Model airfoil (SD7032, solid line) and reference airfoil (FFA-W3-240, dashed line) shapes

The aerodynamic coefficients for the SD7032 for Reynolds numbers equal to 100E3 and 300E3 are available in [14]. However, In order to obtain more dense Reynolds dependency data a new series of wind tunnel tests were performed on a 2D section model of the airfoil. The 2D sectional model is 497mm span-wise long and 130mm chord-wise long and it was manufactured with the same carbon fiber technology used for the turbine blade final model, this ensures the correct reproduction of surface finish effect on the airfoil pefomances, as well as in terms of trailing edge effective thickness.

Tests were carried out at the red wind tunnel facility located at the Lyngby DTU campus (Denmark).

Two aerodynamic coefficients were measured:

- blade section lift coefficient,  $C_l$ , data from the pressure taps drilled in the blade surface
- blade section drag coefficient,  $C_d$ , data from wake rake pressure (the wake rake was present in the DTU wind tunnel and it was placed downstream the model at around 5 chord length)

A total of eight Reynolds number were tested,  $Re=[50E3; 60E3; 75E3; 100E3; 125E3; 150E3; 200E3; 250E3]$ . Fig. 2 shows the obtained aerodynamic coefficient for SD7032 used in the aerodynamic design of the model blade, for different Reynolds numbers, more details about the sectional tests can be found in [15].

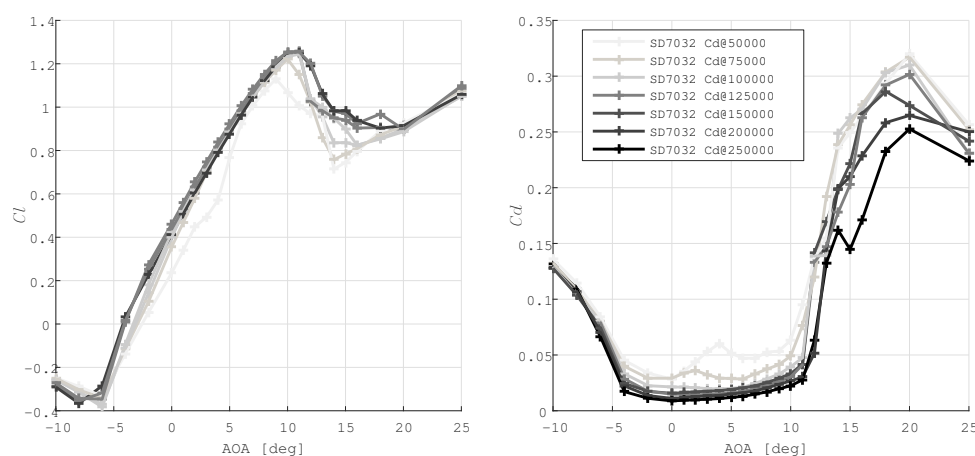


Figure 2: SD7032 lift and drag coefficient from DTU red wind tunnel test

Only the SD7032 was tested since it is the only one used in the model blade design.

### 3.3. Model manufacturing process

In order to match as good as possible, the scaled value for the blade mass and structural response, (i.e. scaled modal frequency) it was decided to employ high performances carbon fiber composite for the model production. The adopted design is quite simple, the blade section is composed of only carbon fiber layer for a total thickness of 0.26 mm. The external shape was guaranteed by the mould thanks to the internal pressure exerted by one balloon that inflates from the inside and it is removed after the autoclave process is completed.

## 4. Design process

Standard turbine rotor design procedures are based on the blade element approach [16, 17], starting from the hypothesis of no radial dependency of the results the design is carried out for each blade section independently. The developed procedure for the wind tunnel model design, herein reported starts from the same blade element approach but instead of merely maximising the rotor aerodynamic performances, i.e. power efficiency, the design objective is the matching of a few selected parameters of the reference full scale turbine. The design optimization loop could be divided in two well separated part. The aerodynamic and the structural part are carried out in tandem and combined within an iterative loop, until the design reaches an optimal solution.

### 4.1. Aerodynamic design

The aerodynamic design deals with the definition of the chord and twist value distribution of the model blade. In order to match the DTU 10MW scaled thrust value, it is necessary to match the scaled lift value along the blade, since in common working condition, the section normal load,  $P_n$ , is generated almost entirely by the section lift, as in Fig. 3.

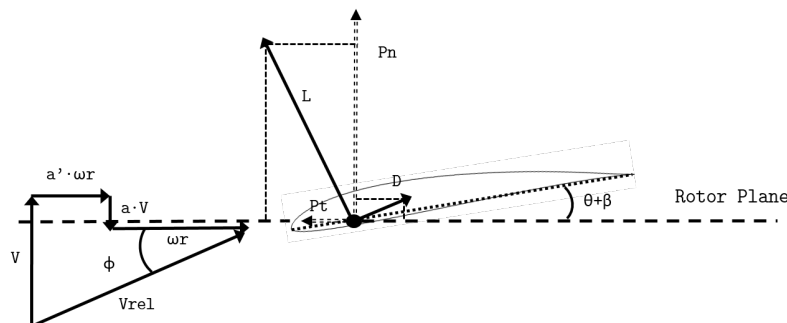


Figure 3: Blade section velocities and loads

The wind tunnel model is successfully designed if the model section lift  $L_{wtm}$  equals the scaled reference one,  $L_{10MW}$ , along the entire blade span, Eq 3.

$$\frac{L_{10MW}}{\Lambda_V^2 \Lambda_L} = L_{wtm} \quad (3)$$

So that it is necessary to consider section lift matching and same working condition for the reference and the model turbine (i.e. same TSR).

The flow angle at full scale and model scale must be exactly the same. It is well accepted [16] to consider the induction factor of the wake,  $a$  and  $a'$  in Fig. 3, only influenced by the lift force and TSR. Thus it is possible to define an unique flow angle  $\phi$  for both the reference and the model turbine, Eq.4. For the model design it was considered the same pitch angle,  $\theta$ , of the reference turbine and two different twist angles,  $\beta_{10MW}$  and  $\beta_{wtm}$ , the angle of attack, AOA,  $\alpha$



is defined consequently in Eq.4.

$$\begin{aligned}\alpha_{10MW} &= \phi - (\theta + \beta_{10MW}) \\ \alpha_{wtm} &= \phi - (\theta + \beta_{wtm})\end{aligned}\quad (4)$$

the Eq.5 comes from the substitution of the lift value in Eq.3 with the lift coefficient,  $Cl$ , times the air dynamic pressure,  $0.5\rho V^2$ .

$$0.5\rho \left(\frac{V}{\lambda_V}\right)^2 Cl_{10MW}(\alpha_{10MW}) \frac{c_{10MW}}{\lambda_L} = 0.5\rho V^2 Cl_{wtm}(\alpha_{wtm}) c_{wtm} \quad (5)$$

The Eq.5 is simplified in Eq.6.

$$Cl_{10MW}(\phi - (\theta + \beta_{10MW})) \frac{c_{10MW}}{\lambda_L} = Cl_{wtm}(\phi - (\theta + \beta_{wtm})) c_{wtm} \quad (6)$$

For pitch regulated turbines in standard working condition it is reasonable to consider that the blade is working far from stall for the most part of its length. Therefore the blade is in the linear aerodynamic region and the lift coefficient can be well approximated with a linear curve with a  $Kl$  slope and  $Cl^0$  zero value, Eq.7.

$$\begin{aligned}Cl_{10MW}(\alpha_{10MW}) &= Kl_{10MW} \cdot \alpha_{10MW} + Cl_{10MW}^0 \\ Cl_{wtm}(\alpha_{wtm}) &= Kl_{wtm} \cdot \alpha_{wtm} + Cl_{wtm}^0\end{aligned}\quad (7)$$

Where  $Kl$  is the lift coefficient first derivative in respect to the angle of attack in the airfoil linear region and  $Cl^0$  is the lift coefficient value at null angle of attack.

Substituting this in Eq.5 the first aerodynamic constraint equation is found, Eq.8

$$(Kl_{10MW} \cdot (\phi - (\theta + \beta_{10MW})) + Cl_{10MW}^0) \cdot \frac{c_{10MW}}{\lambda_L} = (Kl_{wtm} \cdot (\phi - (\theta + \beta_{wtm})) + Cl_{wtm}^0) \cdot c_{wtm} \quad (8)$$

Also the lift derivative in respect to the flow angle,  $\phi$ , is imposed to be matched by the model design, in Eq.9.

$$Kl_{10MW} \cdot \frac{c_{10MW}}{\lambda_L} = Kl_{wtm} \cdot c_{wtm} \quad (9)$$

This is done in order to ensure that the unsteady behaviour of the turbine is well reproduced by the model since the turbine is also going to be tested for unsteady condition [18]. Moreover it is reasonable to consider that, at first approximation, the unsteady behaviour of an aerodynamic body function of the first derivatives of the drag and lift curves calculated around the steady angle of attack [19].

The Eq.8 and Eq.9 can be rearranged in the system equation 10 from which the model chord and twist are computed along the entire blade span.

$$\begin{cases} c_{wtm} = \frac{c_{10MW}}{\lambda_L} \cdot \frac{Kl_{10MW}}{Kl_{wtm}} \\ \beta_{wtm} = \beta_{10MW} - \frac{Cl_{10MW}^0}{Kl_{10MW}} + \frac{Cl_{wtm}^0}{Kl_{wtm}} \end{cases} \quad (10)$$

In Fig. 4 the model airfoil, SD7032, is compared with the DTU 10MW tip airfoil, FFA-W3-240 in terms of lift coefficient  $Cl$  versus angle of attack, for the range  $-2 + 9$ . The lift slope for

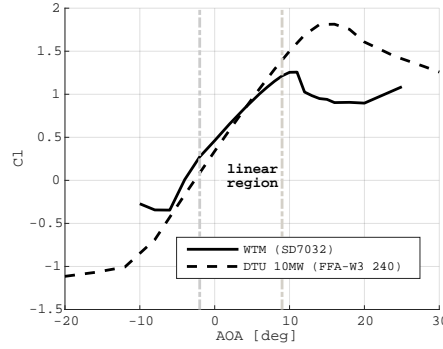
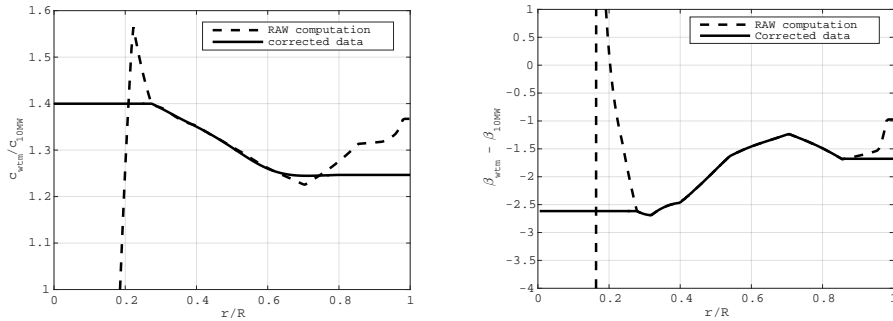


Figure 4: Reference and model airfoil polar lift coefficient comparison

the DTU airfoil is higher than the model one, thus the ratio  $Kl_{10MW}/Kl_{wtm}$  is greater than one which implies a model chord bigger than the geometric scaled reference one.

Fig. 5 shows the the chord and twist design for the DTU 10MW model, Fig. 5a reports the ratio between the model chord and the scaled reference value, Fig. 5b reports the difference between model twist and the reference one. The dashed line are the raw calculation output, the calculation results near the root region were discarded since calculation output seemed inconsistent by visual inspection. Also the tip region design has been simplified to a constant chord and pitch variation also due to manufacturing issues. The chord output was also interpolated with a cubic smoothing spline.



(a) model and scaled 10MW chord ratio (b) model and 10MW twist difference

Figure 5: RAW and corrected output of Eq.10 as function of the non-dimensional blade station

#### 4.2. Structural design

The aerodynamic design defined the chord and twist distribution along the blade span. The remaining degree of freedom is the blade cross section relative thickness ( $t/c$ ) distribution. There are two constraints in the blade relative thickness definition:

- $t/c$  at the blade tip is equal to the nominal  $t/c$  of the SD7032 airfoil ( $t/c=10\%$ )
- $t/c$  must converge to 100% at the blade root to match the circular root section

The blade  $t/c$  is defined in three different regions reported in Fig. 6. Region I is the root region where the blade has a circular cross-section, region III is the tip region, where the cross-

section is the SD7032 profile and lastly in the transition region II the cross-section must converge from the circular shape to the SD7032 shape.

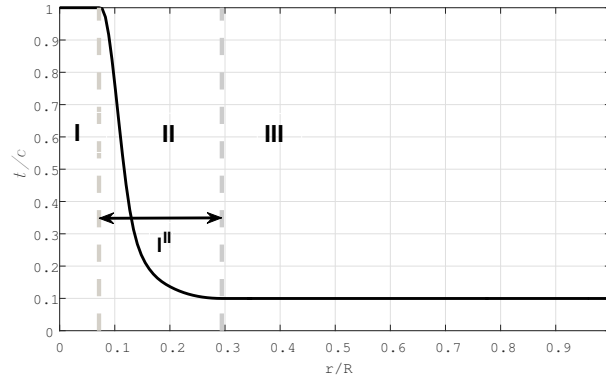


Figure 6: Model blade  $t/c$  definition

The extension of region I was defined by technological constraints, in particular a machined aluminium component has to be glued to blade root in order to allow for the blade assembly. The remaining parameter is the transition region extension,  $l^{II}$ . This dimension has a great impact in the structural performance of the blade, it is obvious that higher  $l^{II}$  means higher model blade stiffness for since the second moment of area of the circular section greater than the SD7032 one.

The  $l^{II}$  length has been numerically optimized in order to ensure the matching of the first scaled flapwise blade frequency (Table 3). A *Matlab*® implemented beam FEM model code was iteratively ran until the correct first flapwise blade modal frequency. The FEM model is discretized by 193 beam elements, for each one the correspondent properties of blade section is assigned, the model is constrained as a cantilever beam in order to compute the modal analysis.

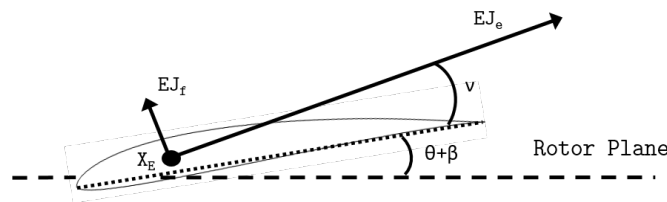


Figure 7: Definition of the blade structural principal axes (not in scale).

As reported In Fig. 7, from a structural point of view, the blade section is characterized by:

- $EJ_1(N \cdot m^2)$  bending stiffness about the first principal axis, flapwise direction
- $EJ_2(N \cdot m^2)$  bending stiffness about the second principal axis,edgewise direction
- $X_E(m)$  elastic section center
- $\nu(rad)$  principal axes orientation in respect to the chord line
- $m(kg/m)$  mass per unit length

At this design phase the blade was considered made only by unidirectional high modulus carbon fiber layer aligned with the blade radial direction. Discarding the anisotropy in the material the elastic modulus and density of the carbon fiber was taken from standard commercially available data,  $E = 135MPa$ ,  $\rho = 1560kg/m^3$ , one layer of carbon fiber was considered for a total of thickness of 0.26mm. Knowing the material properties and thickness and considering the blade

chord and twist output from the aerodynamic design the blade section mechanical properties are easily computed, see [16] for theoretical details.

Once the  $l^{II}$  length is optimized, the t/c blade profile is completely defined, the last phase of the structural design is the recalculation of the blade section shape and aerodynamic coefficient. In region I and region III the section shape and aerodynamic are perfectly known, being respectively equal to the circular section and SD7032 section. In region II the section shape and aerodynamic coefficients are calculated as function of the radial position from simple linear interpolation based on the t/c local value. In Fig. 8 the section shape and lift coefficient is shown for four different, sample, radial blade positions.

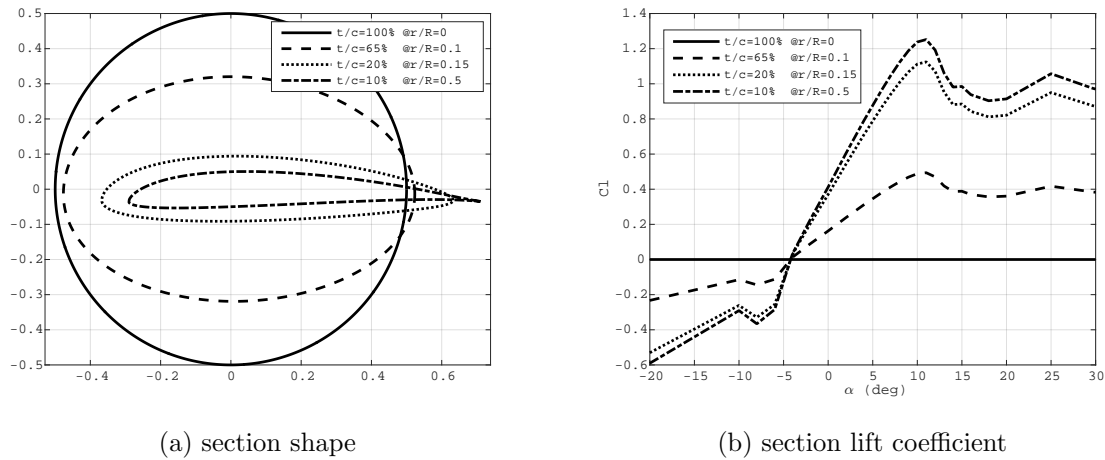


Figure 8: Blade shape and lift coefficient at different radial position and t/c

#### 4.3. Design Loop

The aerodynamic and structural design are part of an iterative loop the steps of which could be summarized as:

- (i) Compute model airfoil  $Kl_{wtm}$  and  $Cl_{wtm}^0$  from model section lift coefficient
- (ii) Calculate model chord and twist from Eq.10
- (iii) Estimate section mechanical properties
- (iv) Optimize  $l^{II}$  for blade flapwise frequency
- (v) Update blade section shape and lift coefficient and loop from (i)

The design is considered finished when the  $l^{II}$  variation from one iteration to the following is below a 5% threshold. Fig. 9 shows the output of four subsequent iterations, the design starts from the DTU 10MW reference value for chord, twist and t/c then the optimized solution is computed, it is visible how the chord grows higher than the fullscale reference, in particular near the maximum chord position, the twist is almost equally reduced along the blade by a couple of degrees and the t/c curve goes faster to the tip airfoil thickness than the 10MW one.

#### 4.4. Blade shape export to CAD file

From the chord, twist and t/c distributions the blade shape is entirely known, at first step the blade is generated as a point cloud generated by 721 points at 193 different blade radial positions. From the point cloud using a 3D B-Spline space interpolation the blade shape was exported to iges file format based on an in-house *Matlab*® blades converter in order to make the manufacturing process easier.

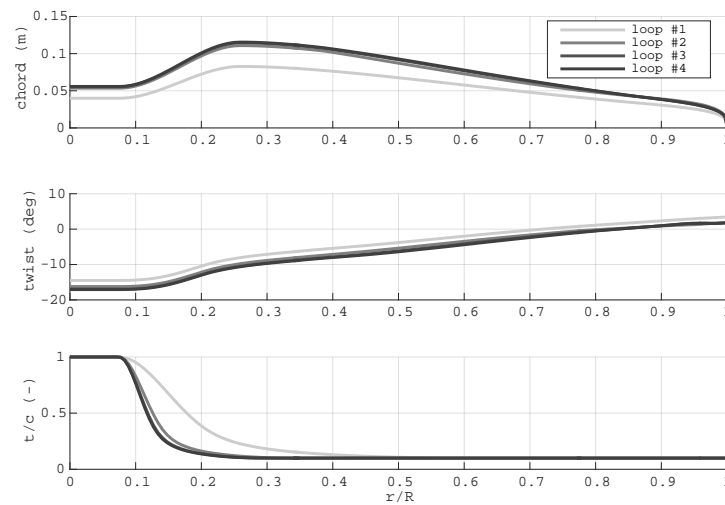
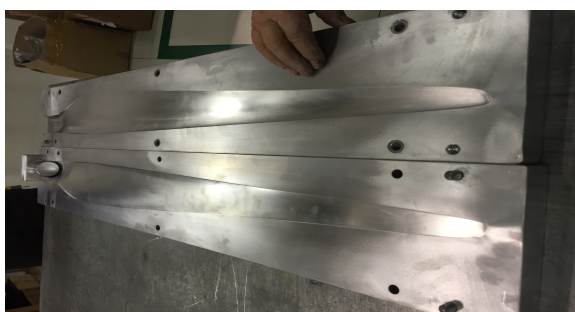


Figure 9: Output of the design algorithm at different iteration loop as chord, twist and t/c value vs the non dimensional blade radial position

## 5. Blade production

From the blade CAD file a CNC machined mould has been realized, Fig. 10a. A first blade prototype, Fig. 10b, was realized with prepreg using a vacuum bag oven process, the mould is divided in two part that are the pressure and suction side of the blade, the blade layers are placed in the mould and pushed against the mould surface with an inflated plastic balloon. This first blade prototype was made with a different carbon fiber specifications compared to the output of the aeroelastic design, this since the first set of tests, linked to LIFES50+ deliverable 3.1 (Dev3.1) [1], had the main purpose of characterizing the aerodynamic behaviour only, for this tests the elastic response was not of primary interest.



(a) aluminium mould



(b) carbon fiber blades

Figure 10: blade manufacturing

At the time of writing this paper, the aeroelastic blades are being manufactured according to the optimal design specification.

## 6. Wind tunnel tests and conclusion

Fig.11 shows the results of the wind tunnel model compared to the scaled DTU 10MW performance in terms of thrust and torque. The agreement on the thrust force is excellent

for all the tested conditions, the maximum thrust force,  $\sim 70N$ , is well reproduced by the turbine model. Also the torque matching, that was not the main model target, is very good up to the rated condition, only at the 8 m/s point there is a lower wind tunnel torque than the reference value.

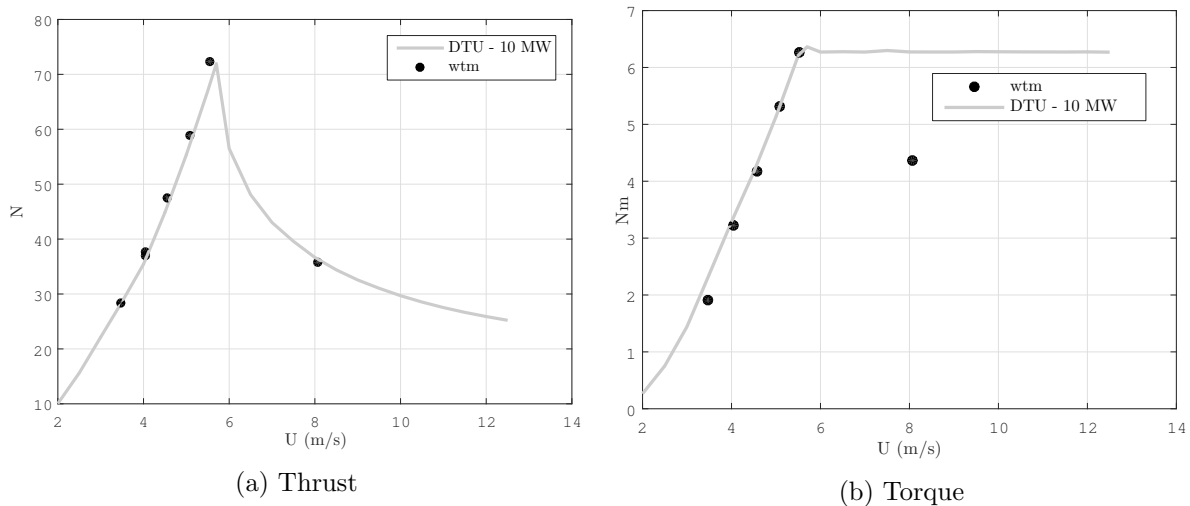


Figure 11: Wind tunnel model (wtm) test results compared with the reference scaled DTU 10MW performances

However the rotor used during the presented tests adopted a manual pitch regulation mechanism that made not possible a fine adjustment of blade pitch angle. Ongoing development of the turbine hub design [20] will be adopting harmonic drive actuators connected to the blade root allowing an angular position resolution in the order of hundredths of degree. The improvement in the pitch precision will allow to refine the matching of the reference curve. Thus, depending on the application, the most interesting parameter to be matched could be the rotor thrust or torque, e.g. for floating turbine testing is the thrust or for wind farm efficiency is the torque.

In conclusion, the design of the wind tunnel rotor was satisfactory in terms of the aerodynamics performance, in particular considering that the main target of the design was the matching of the DTU 10MW thrust curve.

A further ongoing improvement of the turbine model is related to the blade structural characterization, the first blade prototype adopted in this tests does not follow exactly the specification from the optimal design, since only the aerodynamic performances were the objective of this first test session. By the time of this writing the aeroelastic version of the blade are being manufactured with more strict technological specifications regarding the fiber layup orientation and thickness. Afterwards the modal response will be measured in order to characterize the dynamic properties of manufactured blades.

## References

- [1] <http://lifes50plus.eu>
- [2] C. Bak et Al, The DTU 10-MW Reference Wind Turbine, Technical University of Denmark, DTU Wind Energy, Denmark, 2013.
- [3] H. Bredmose, "Contribution to InnWind Deliverable 4.22, Scaling laws for floating wind turbine testing". DTU Wind Energy. 2014
- [4] C. Bottasso, F. Campagnolo & V. Petrovic. "Wind tunnel testing of scaled wind turbine models: Beyond aerodynamics." Journal of Wind Engineering and Industrial Aerodynamics, 2014

- [5] F. Campagnolo, C. Bottasso & P. Bettini "Design, manufacturing and characterization of aero-elastically scaled wind turbine blades for testing active and passive load alleviation techniques within a ABL wind tunnel.", TORQUE, 2014
- [6] M. Make. "Predicting scale effects on floating offshore wind turbines." MsC thesis, TUDelft, 2014
- [7] H. Bredmose, R. Mikkelsen, A. M. Hansen, R. Laugesen, N. Heilskov, B. Jensen, & J. Kirkegaard. "Experimental study of the DTU 10 MW wind turbine on a TLP floater in waves and wind". EWEA Offshore 2015 Conference, Copenhagen, 2015
- [8] E. Bachynski, V. Chabaud, T. Sauder, Real-time Hybrid Model Testing of Floating Wind Turbines: Sensitivity to Limited Actuation, Energy Procedia, Volume 80, 2015.
- [9] I. Bayati, M. Belloli, A. Facchinetti, and S. Giappino. Wind tunnel tests on floating offshore wind turbines: A proposal for hardware-in-the-loop approach to validate numerical codes. Wind Engineering, 2012.
- [10] I. Bayati, M. Belloli, D. Ferrari, F. Fossati, and H. Giberti. Design of a 6-dof robotic platform for wind tunnel tests of floating wind turbines. Energy Procedia, 2014.
- [11] C. Bak, R. Bitsche, A. Yde, T. Kim, M. H. Hansen, F. Zahle, ... T. Behrens. "Light Rotor: The 10-MW reference wind turbine". Proceedings of EWEA 2012 - European Wind Energy Conference. European Wind Energy Association (EWEA), 2012.
- [12] J. Jonkman, S. Butterfield, W. Musial, G. Scott. Definition of a 5-MW Reference Wind Turbine for Offshore System Development. Technical Report NREL/TP-500-38060, NREL National Renewable Energy Laboratory, 2009.
- [13] A. Zasso, S. Giappino, S. Muggiasca, L. Rosa "Optimization of the boundary layer characteristics simulated at Politecnico di Milano Boundary Layer Wind Tunnel in a wide scale ratio ranges". IRIS Politecnico di Milano, 2005.
- [14] C. A. Lyon, A. P. Broeren, P. Gigure, A. Gopalarathnam, and M. S. Selig, "Summary of Low-Speed Airfoil Data, Vol. 3", SoarTech Publications, Virginia Beach, VA, 1998
- [15] [http://lifes50plus.eu/wp-content/uploads/2015/11/GA\\_640741\\_LIFES50\\_D3.1-merged.pdf](http://lifes50plus.eu/wp-content/uploads/2015/11/GA_640741_LIFES50_D3.1-merged.pdf)
- [16] M. O. L. Hansen, "Aerodynamics of Wind Turbines : second edition. 2 ed.", Earthscan Publications Ltd, 2008.
- [17] J. Manwell, J. McGowan and A. Rogers, "Wind Energy Explained: Theory, Design and Application", Second Edition, John Wiley & Sons, Ltd, 2009
- [18] I. Bayati, M. Belloli, L. Bernini, A. Zasso. "Wind tunnel validation of AeroDyn within LIFES50+ project: imposed Surge and Pitch tests", Journal of physics conference series, The Science of Making Torque from Wind, 2016.
- [19] F. Cheli, G. Diana, "Advanced Dynamics of Mechanical Systems", Springer, 2015
- [20] I. Bayati, M. Belloli, L. Bernini, E. Fiore, H. Giberti, A. Zasso, "On the functional design of the DTU10 MW wind turbine scale model within LIFES50+ project", Journal of physics conference series, The Science of Making Torque from Wind, 2016.